

## On-Orbit Performance of the ACS Solar Blind Channel

Hien D. Tran, Gerhardt Meurer, Holland C. Ford, Andre Martel, Marco Sirianni  
*Dept. of Physics & Astronomy, The Johns Hopkins University, Baltimore, MD  
21218*

Ralph Bohlin, Mark Clampin, Colin Cox, Guido De Marchi, George Hartig  
*Space Telescope Science Institute, 3700 San Martin Drive, Baltimore, MD 21218*

Randy Kimble  
*Goddard Space Flight Center, Code 681, Greenbelt, MD 20771*

Vic Argabright  
*Ball Aerospace, Boulder, CO 80301*

**Abstract.** The ACS solar blind channel (SBC) is a photon-counting MAMA detector capable of producing two-dimensional imaging in the UV at wavelengths 1150–1700 Å, with a field of view (FOV) of  $31'' \times 35''$ . We describe the on-orbit performance of the ACS/SBC from an analysis of data obtained from the service mission observatory verification (SMOV) programs. These data show that the detector is behaving nominally. Images of stars with the SBC reveal an aberration in the optics similar to that observed in the HRC at UV wavelengths.

### 1. Introduction

The Solar Blind Channel (SBC) of the Advanced Camera for Survey (ACS), installed in March 2002 on the *Hubble Space Telescope (HST)* during Service Mission 3B (SM3B) is a spare detector from the Space Telescope Imaging Spectrograph (STIS) program. It is a Multi-Anode Microchannel Array (MAMA) photon-counting device that uses a CsI photocathode on a curved microchannel plate (MCP). To improve the quantum efficiency, the MAMA detector has been equipped with a field electrode, or repeller wire, that repels electrons emitted away from the MCP back into the channel. Optimized for UV imaging at wavelengths 1150 Å to 1700 Å, the SBC has an imaging area of  $1024 \times 1024$  pixels with a sampling of  $0.030''$  per pixel, yielding a total field of view of  $31'' \times 35''$ . Besides a set of long-pass filters (F115LP, F125LP, F140LP, F150LP, F165LP), and a Ly $\alpha$  (F122M) filter for direct imaging, it is also equipped with two prisms for low-resolution ( $R \sim 100$ ) objective prism spectroscopy. The detector is cosmetically fairly clean, the only defects being a broken anode and three small clusters of hot pixels. As with the STIS MAMA detector, the ACS/SBC has bright-object limits to protect it from radiation damage. For non-variable sources, the local (per pixel) count rate cannot be over 50 counts/sec/pixel, and the global (over the whole detector) limit is  $< 2 \times 10^5$  counts/s. The optical performance of the SBC is comparable to that of the STIS FUV-MAMA. The ACS/SBC is expected to give slightly higher quantum efficiency but lower S/N due to higher dark current than the STIS FUV-MAMA. Since launch, a number of tests for performance characterization of ACS have been carried out as part of the service mission observatory verification (SMOV) program. We briefly report here the results of some of these tests for the SBC. Some discussion of the

ACS imaging quality is also given in Hartig et al. (2002), and the geometric distortion in the ACS detectors is described by Meurer et al. (2002).

## 2. SMOV Results

Observations of the globular star cluster NGC 6681 were used to characterize many of the SBC properties, including flux calibration, geometric distortion, low-order flat creation, PSF, and monitoring of contamination.

### 2.1. Detector Health

An important SBC diagnostic is the so-called “fold analysis.” Individual photon events generate charge clouds which impinge on the position-sensing anode array. The number of anode lines that collect a charge signal is the “fold number” for the event. The distribution of fold numbers measures the gain distribution for the MCP. A shift to lower fold numbers would imply gain sag in the MCP, perhaps due to excessive accumulated illumination, while a shift towards larger fold number pulses could indicate leakage of gas into or production of gas within the sealed detector tube. Comparison of event distributions observed during ground testing of the tube in 1997 and more recently in-flight shows that there is little change in the distributions over a period of  $\sim$  four years. This indicates that the detector is in fairly good health.

### 2.2. Dark Currents

The first in-flight observations for a “super dark” image were taken over a ten hour span, near the maximum time between South Atlantic Anomaly passages. The mean dark rate in this image is  $1.049\text{e-}5$  counts/sec/pixel = 0.0378 counts/hour/pixel. This fairly low rate is comparable to those measured during the thermal vacuum ground calibration campaign of July 2001 (Martel et al. 2001), and is largely due to a relatively cool tube temperature  $T_{SBC} = 15^\circ$  to  $27^\circ$  C during the observations. Ground thermal modeling indicates that a thermal balance at  $T_{SBC} = 35^\circ$  to  $37^\circ$  C may occur, in which case the dark rate will be about three times higher.

### 2.3. Image Quality

Figure 1 illustrates the PSF structure in SBC images. The right-hand panel shows an encircled energy (EE) curve and a radial profile of a star in the first light data. The solid curves show the profiles at nominal  $x$ -scale, whereas the scale has been stretched by a factor of ten for the dashed curves. The EE curve shows that 28% of the light is contained within a circular aperture  $0.12''$  in diameter, while 51% of the light is contained within a diameter of  $0.25''$ . The left hand panel expands a portion of the F125LP first light image. These data have been corrected for geometric distortion. There is a small spur extending  $\sim 0.13''$  from the center of each PSF to the lower right. This is due to aberration in the system. A similar aberration is seen in UV images of the high resolution channel (HRC), but the aberration is not seen at optical wavelengths with either HRC or the wide field channel (WFC; Hartig et al. 2002).

### 2.4. Sensitivity

The SMOV data indicate that the SBC throughput is very close to pre-launch expectations. In Figure 2 we show the average ratio of the observed over expected count rates for 10 different stars in NGC 6681, whose spectra are well-known from STIS spectroscopy, as a function of wavelength. The on-orbit data were measured within a  $0.4''$  radius aperture. Data for the F122M ( $\text{Ly}\alpha$ ) filter came from the standard star HS+2027. Except for F165LP, the sensitivity of the SBC is very close to expectations. The  $\sim 16\%$  increase in sensitivity

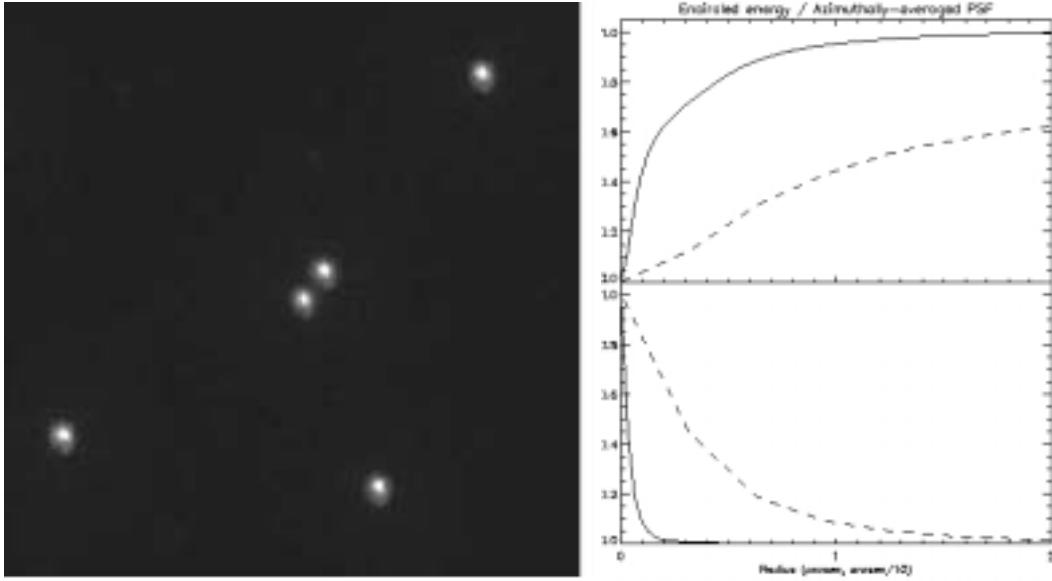


Figure 1. ACS/SBC PSF profile (*right bottom*) and encircled energy curve (*right top*). The left panel shows the low-level elongation to the lower right in the PSF of each star due to aberration.

in the F122M band is probably not a result of higher efficiency of the detector, but may be due to red leak.

## 2.5. Contamination Monitor

The UV sensitivity of the ACS/SBC MAMA detector was monitored approximately once a week for the first two months, and once a month thereafter, using observations of a field in the globular cluster NGC 6618. This field contains several stars well-observed with STIS for its own UV sensitivity monitoring program. The SBC observations were made through all five longpass filters (F115LP, F125LP, F140LP, F150LP, F165LP).

The results of the UV contamination monitor show that the observed count rates are quite stable, and behave nominally for all SBC filters. Figure 3 shows that the count rates measured within a  $0.6''$  radius aperture do not change significantly during the six epochs over the first 72 days that the SBC UV fluxes were monitored. We conclude from this behavior, and from the throughput comparison with STIS, that the SBC optics suffered no degradation in throughput resulting from any contamination during the service mission.

**Acknowledgments.** ACS was developed under NASA contract NAS5-32864, and this work was supported by a NASA grant.

## References

- Hartig, G. F., et al. 2002, in *Future EUV and UV Visible Space Astrophysics Missions and Instrumentation*, eds. J. C. Blades & O. H. Siegmund, Proc. SPIE, Vol. 4854, in press [4854-30]
- Martel, A. R., Hartig, G., & Sirianni, M. 2001, [http://acs.pha.jhu.edu/instrument/calibration/results/by\\_item/detector/sbc/darks\\_jul01/](http://acs.pha.jhu.edu/instrument/calibration/results/by_item/detector/sbc/darks_jul01/)
- Meurer, G. R., et al. 2002, in *Future EUV and UV Visible Space Astrophysics Missions and Instrumentation*, eds. J. C. Blades & O. H. Siegmund, Proc. SPIE, Vol. 4854, in press [4854-30]

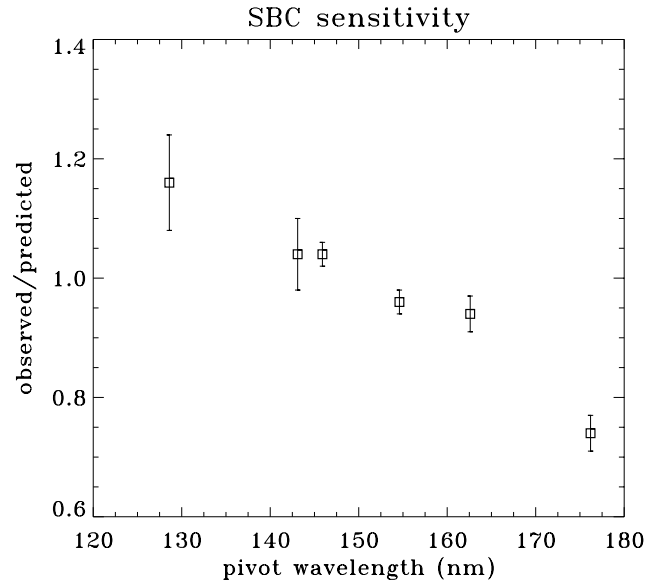


Figure 2. Average observed/predicted count rate ratios of 10 different stars in NGC 6681 as a function of SBC bandpasses. In order from left to right, the filters are: F122M, F115LP, F125LP, F140LP, F150LP, F165LP.

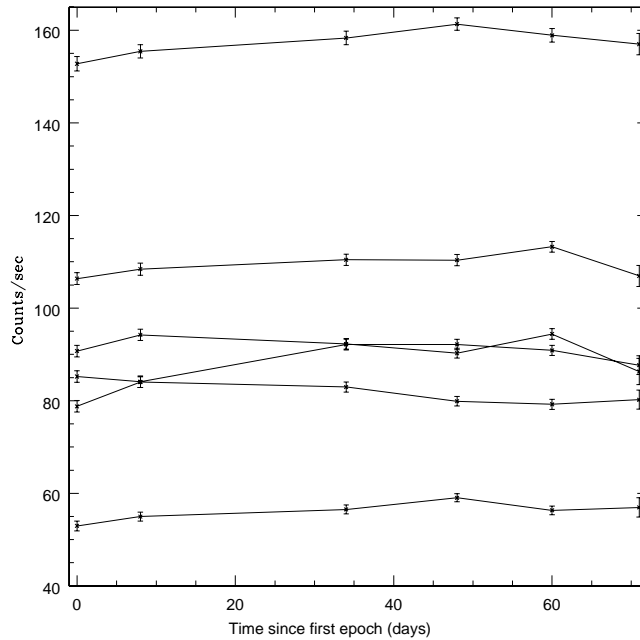


Figure 3. Count rates versus time for six different stars in NGC 6681 through the F115LP filter of SBC. Similar behavior is seen for other filters. No significant changes in count rates are seen as a function of time over the first two months of monitoring.